Proceedings of the 21st ICSMGE, Vienna, Austria, 14 – 19 June 2026. Pistrol, Adam & Schweiger (eds.)
Published by: ÖGG, Austrian Society for Geomechanics, Salzburg, Austria, ISBN 978-3-9503898-4-5
https://doi.org/10.53243/ICSMGE2026-134

The effect of chemical stabilization on the behavior of slopes during shaking

Aly Ghanem, Mohamed I. Amer, **Shehab S. Agaiby**
Cairo University, Faculty of Engineering, Public Works Department, Giza, Egypt: shehabagaiby@cu.edu.eg

ABSTRACT: Numerous embankments and slopes sustained significant damage during prior earthquakes, resulting in both economic and human losses. Prior studies mostly concentrated on mechanical reinforcement techniques, such as geogrids and soil nailing, to enhance the slope's performance during seismic activities. Prior studies and field observations indicate that these techniques enhance slope stability by mitigating deformations induced by seismic activity. Nonetheless, these methods may incur significant expenses in certain instances. The impact of chemical stabilization with cement on the slope's behavior during shaking is examined to identify a more cost-effective approach. A series of 1-g shake table experiments was conducted on slopes with varying cement concentrations under different surcharge loadings at the crest. The behavior was evaluated by observing the acceleration amplification along the slope's elevation and the consequent crest subsidence. Results indicate that employing minimal amounts of cement enhances the slope's resistance to elevated seismic energy before failure, reduces crest settlement, and confines failure to the top sections of the slope, rendering it a feasible solution for slope and embankment stabilization.

KEYWORDS: chemical stabilization, slope stability, Portland cement, dynamic behavior, 1-g shake table

1 INTRODUCTION

The rapid expansion of urban development continues to reduce the availability of land for infrastructure projects. As a result, practitioners are often required to identify alternative design solutions that meet project requirements while conforming to increasingly restrictive spatial constraints. One of the most commonly encountered challenges in urban construction is the limited space available for building embankment roads. These spatial limitations, often due to nearby existing structures or property boundaries, can necessitate constructing slopes with angles steeper than those that clean, cohesionless sand can naturally support. In such cases, additional reinforcement measures are essential to ensure slope stability and to prevent failure.

To address this issue, a range of soil stabilization techniques has been implemented in geotechnical engineering practice, broadly categorized into mechanical and chemical methods. Mechanical stabilization—such as the use of geosynthetics or soil nails adds reinforcing elements to the soil mass, enhancing the system's overall resistance through improved frictional and cohesive interactions (Madhavi Latha and Nandhi Varman, 2014; Ayazi and Tangri, 2022; Mollaei et al., 2022). While mechanical solutions are effective, they may be unnecessarily complex or costly in projects where only moderate slope steepening is required. In such instances, chemical stabilization provides a practical and cost-effective alternative.

Chemical stabilization involves the introduction of chemical binders that enhance the strength and stiffness of soils by promoting particle bonding and cohesion (Shooshpasha and Shirvani, 2015). Among the wide variety of chemical additives available, Portland cement is widely recognized as one of the most effective stabilizers for clean sandy soils. Numerous element-scale experimental studies have investigated the effect of cement content on the mechanical behavior of sand–cement mixtures. For instance, Consoli et al. (2007) and Rios (2011) conducted unconfined compression tests to evaluate the influence of cement content (CC) on the strength of sand-cement mixtures. Their results showed that the unconfined compressive strength increased by a factor of 4.5-6.0 as the cement content increased from 1% to 7%, depending on the initial dry density. Wang and Leung (2008) employed triaxial testing to evaluate mixtures with cement contents ranging from 1% to 3%, observing a progressively dilative behavior with an approximate twofold increase in peak strength as the cement content increased from 0% to 3%.

Additionally, Saxena et al. (1988) examined the low-strain stiffness and damping properties of cemented sands using resonant column tests. Their results indicated that at low cement contents (up to ~2%), the dynamic moduli increased slightly, alongside a corresponding increase in damping ratios. Beyond this threshold, a significant increase in dynamic moduli was observed, while the damping ratios remained relatively unaffected.

To bridge the gap between material-level understanding and system-level performance, this research undertakes a comprehensive investigation into the effects of cement stabilization on the dynamic behavior of sand slopes. The study transitions from laboratory testing of material properties to a system-level analysis by employing a series of physical model tests. This approach enables a more realistic assessment of how cement treatment affects the overall stability and response of a slope under seismic loading.

A total of eleven 1-g shake table experiments were meticulously designed and executed to simulate earthquake conditions on clean sand slopes. These experiments form the core of the study, providing valuable data on the dynamic response of the treated slopes. The experimental program was structured to systematically evaluate the influence of two critical parameters: cement content and surcharge loading at the slope crest. The variation in cement content allows for a direct assessment of its effectiveness in improving slope stability. At the same time, the surcharge loading is introduced to amplify the driving forces, thereby simulating more severe seismic scenarios and pushing the slopes closer to failure.

By systematically varying these parameters, the study aims to provide a detailed understanding of the complex interplay between cementation, seismic loading, and slope response. The findings from these experiments are expected to offer significant insights into the efficacy of cement stabilization as a ground improvement technique for enhancing the seismic performance of sand slopes and to provide a basis for the development of more robust design guidelines.

2 MODEL SETUP AND EXPERIMENTAL PROGRAM

2.1 *Equipment*

Shake table tests were conducted using a uniaxial seismic simulator at the Soil Mechanics and Foundations Research Laboratory at Cairo University. The system includes a 1.5 m × 1.5 m steel platform driven by a servo-hydraulic actuator and controlled via a displacement-based control system. A rigid

model container measuring 1.1 m × 1.1 m × 1.0 m was mounted on the platform to house the slope models. Further details regarding the equipment used and the experimental setup are provided in Ghanem (2023).

2.2 *Soil Properties*

The selection and characterization of the constituent materials were foundational to this experimental study. The base soil used was locally obtained sand, which was classified as poorly graded (SP) based on its particle-size distribution. Sieve analysis indicated a uniformity coefficient (Cu) of 2.3 and a fines content of 2.3%, confirming a narrow particle-size distribution. This characteristic is significant because it influences soil packing density, permeability, and overall mechanical behavior, particularly its susceptibility to dynamic loading.

To ensure consistent and repeatable preparation of the slope models, a comprehensive suite of standard geotechnical laboratory tests was conducted to determine the engineering properties of the sand. Standard Proctor compaction tests were performed to determine the material's compaction characteristics, yielding a maximum dry density of 1775 kg/m³ at an optimum moisture content of 11.6%. These values provided the benchmark for compacting the sand in the model tests. The shear strength of the sand was quantified through a series of direct shear tests conducted on samples prepared to 95% of the maximum Proctor density. These tests determined the effective friction angle to be 35.5°, a critical parameter for evaluating the inherent stability of the uncemented slope. For the stabilization component of the study, a commercially available Portland pozzolanic cement was used as the binding agent. This cement type is commonly employed in ground improvement projects due to its favorable hydration properties and long-term strength development. The cement was introduced at varying percentages by dry weight of the sand to create the stabilized slope models. For a more exhaustive description of the material properties and the testing procedures followed, readers are referred to the detailed documentation provided by Ghanem (2023).

2.3 *Model Configurations*

Eleven shake table tests were conducted using a 1:6 model-to-prototype scale factor. All quantities reported herein refer to the model scale. Prototype-scale values can be estimated using the scaling relationships outlined by Iai (1989).

The tests were grouped into three groups based on their cement content, with the variable in each group being the surcharge applied at the slope crest. Cement contents of 1%, 2%, and 3%, and surcharge values of 0, 1.0 kPa, and 1.5 kPa were considered. All slopes had a slope angle of 1.25H:1V and a total height of 30 cm. For cemented slopes, a water content of 1% was used to ensure full hydration of the binder, and the models were cured for four days prior to testing.

Table 1. Summary of testing configurations

	Group (1)			Group (2)			Group (3)			Group (4)	
Test No.	01	02	03	04	05	06	07	08	09	10	11
Cement Content "CC" (%)	0			3			1			2	
Surcharge "q" (kPa)	0	1.0	1.5	0	1.0	1.5	0	1.0	1.5	0	1.5

A comprehensive instrumentation scheme was implemented to monitor the dynamic response of the model slopes during shaking. This setup was designed to capture both the input ground motion and the resulting behavior of the slope body, including internal acceleration, crest displacement, and visual failure mechanisms.

The primary measurement of seismic response was achieved using a set of five accelerometers. One accelerometer (A0) was securely mounted on the shake table platform to provide a precise record of the input motion imparted to the model's base. The remaining four accelerometers (A1–A4) were strategically embedded within the sand slope itself to monitor the propagation and amplification of seismic waves. These sensors were positioned at relative heights of 0, 0.3, 0.6, and 0.9 from the base of the slope. To specifically target the anticipated shallow failure zone, all four embedded accelerometers were placed at a horizontal distance of 6 cm from the slope face. This arrangement enabled detailed tracking of the internal dynamic response throughout the slope's height.

In addition to acceleration, crest displacement was continuously monitored using a Linear Variable Differential Transformer (LVDT). The LVDT was mounted on a rigid steel angle bracket adjacent to the slope crest, allowing for accurate measurement of permanent and transient deformations. To ensure data integrity and minimize three-dimensional boundary effects from the container, all electronic sensors, including the accelerometers and LVDTs, were aligned along the model's central longitudinal axis. The complete layout of the slope geometry and instrumentation is detailed in Figure 1.

Finally, to supplement the quantitative data, visual observations of the slope's performance were recorded throughout each experiment. A high-resolution camera was mounted on a tripod to the side of the transparent container, capturing the development of failure surfaces and overall deformation patterns during shaking. This qualitative data provides critical context for interpreting the sensor measurements and understanding the failure mechanisms.

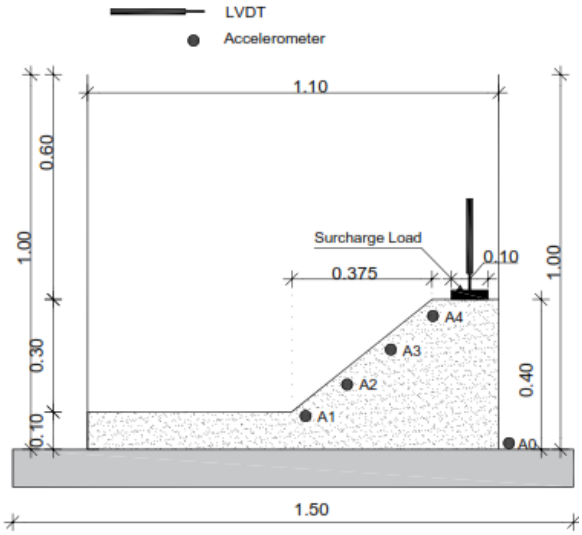

Figure 1. Model configuration and instrumentation layout

2.4 *Input Ground Motion*

To ensure consistent, repeatable assessment of slope performance, a standardized input ground motion was applied across all experiments. The selected waveform consisted of tapered sine waves with a fixed frequency of 3 Hz. Based on the scaling laws applicable to 1-g shake table testing, this model-scale frequency corresponds to approximately 1.22 Hz at the prototype scale, representing a realistic seismic frequency. The use of a controlled, synthetic waveform allows for a clear investigation of the system's response without the inherent variability of natural earthquake records, ensuring that differences in performance can be directly attributed to the parameters under investigation, namely cement content and

surcharge loading.

The loading protocol was designed to increase the seismic demand on the slope models incrementally. For the initial test series (Groups 1 to 3), the motion amplitude was set at 0.1g and progressively increased to a maximum planned amplitude of 0.6g. However, since failure was not observed in the cemented slopes of Group 2 under this loading regime, a procedural adaptation was made for Group 4. For this final group, the maximum amplitude was extended to 0.8g to ensure that the failure threshold could be reached and the ultimate capacity of the stabilized slope could be assessed. Each loading step followed a consistent time history: the acceleration was ramped up from zero to the target amplitude over a two-second interval, maintained at a steady state for six seconds, and then ramped back down to zero over two seconds. A complete time history of the input motion is illustrated in Figure 2.

To provide a quantitative measure of the seismic energy imparted to the slopes during each test, the Arias Intensity was adopted as the primary energy-based metric. Arias Intensity is calculated by integrating the squared acceleration over the entire duration of the ground motion, providing a robust, comprehensive measure of the shaking's total energy content. This metric was used to assess and compare the cumulative energy required to induce failure in the slopes under different experimental conditions with varying surcharge loads and cement contents, offering valuable insights into the effectiveness of the stabilization treatment.

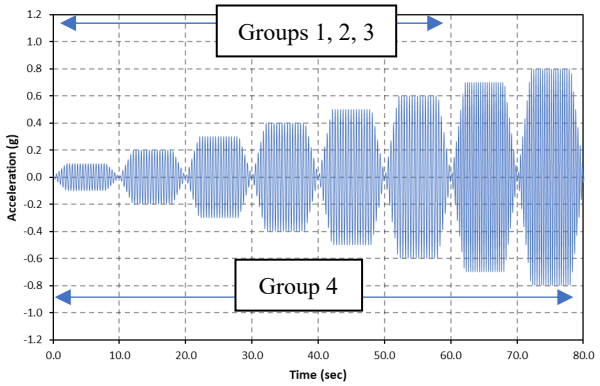

Figure 2. Applied ground motion for different groups

3 RESULTS

The effects of surcharge loading and cement content on the dynamic response of semi-dry sand slopes were evaluated. Results are presented in terms of (i) the variation of the amplification factor with peak ground acceleration (PGA) at different relative heights within the slope, (ii) the crest settlement as a function of PGA, and (iii) the Arias intensity required to initiate failure. Photographic documentation taken before and after each test was used to qualitatively validate the instrument-recorded data. Slope failure was identified at the instance when a notable drop in the amplification factor occurred, indicating localized failure near the corresponding accelerometer. Global slope failure was considered to occur when any point within the slope exhibited signs of instability. The Arias intensity corresponding to the slope failure instance was computed for each test and compared across different cement contents and surcharge levels. This comparison enabled assessment of the influence of cement stabilization and surcharge loading on the energy-absorption capacity of the slopes.

3.1 *Amplification Factors*

To analyze the internal dynamic response of the slope models, an amplification factor was employed. This factor provides a quantitative measure of how the input ground motion is modified as it propagates upward through the soil mass. For any given relative height within the slope, the amplification factor is formally defined as the ratio of the peak acceleration recorded by the accelerometer at that elevation to the peak acceleration recorded by the reference accelerometer at the base of the model. This normalization allows direct comparison of the seismic response at different levels within the slope, highlighting zones of significant ground-motion amplification or de-amplification.

The primary application of this analysis in the current study is to serve as an indirect method for identifying the onset and location of internal failure mechanisms. The methodology involves tracking the variation of the amplification factor at each sensor location as the peak ground acceleration (PGA) of the input motion is incrementally increased. By plotting the amplification factor against the input PGA for each accelerometer (A1-A4), a response curve is generated that illustrates the evolution of the dynamic behavior at different depths within the slope under progressively more vigorous shaking.

The interpretation of these response curves provides critical insights into the stability of the slope. In a stable, intact soil mass, the amplification factor is expected to follow a relatively consistent trend. However, the development of a shear failure plane causes a distinct and significant drop in this relationship. This sudden decrease in amplification occurs because the soil mass containing the accelerometer becomes kinematically decoupled from the underlying stable portion of the slope. Once this separation happens, the transmission of shear waves to the detached block is impaired, leading to a reduction in its measured acceleration relative to the input base motion. Therefore, a sharp decline in the amplification factor at a specific sensor location is a robust indicator that a local failure has initiated at or below that depth.

Results for Test No. 03 and 06 are shown in Figure 3a-b as an example. The amplification factor initially remains stable with increasing PGA, then shows a slight increase before suddenly dropping, indicating failure. These trends are consistent with previous studies conducted on similar slopes (Yang et al., 2018; Zhou et al., 2019; Hazari et al., 2020). When no cement is used, failure occurs at relative heights of 0.6 and 0.9 at 0.4g and 0.5g, respectively. However, with a 3% cement content (T06), no drop is observed, indicating that no failure occurred at any relative height.

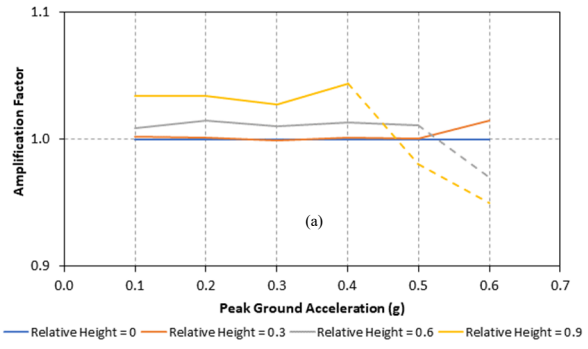

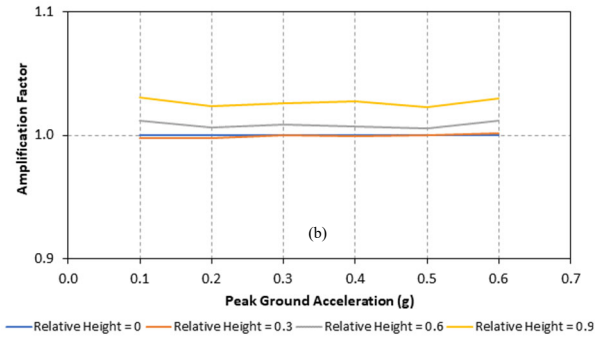

Figure 3. Variation of amplification factor with PGA at different relative heights for (a) Test No. 03 and (b) Test No. 06

3.2 *Energy required to initiate failure*

The precise identification of failure initiation is a critical step in interpreting the experimental results. For this study, the instance of failure is defined as the moment corresponding to the first significant and irreversible drop in the amplification factor recorded at any of the embedded accelerometers. This criterion provides a consistent and objective method for pinpointing the onset of internal shearing and the formation of a failure plane within the slope model.

To illustrate the application of this methodology, the results from test T03 are presented as a representative example. By plotting the amplification factors for each accelerometer against increasing peak ground acceleration (PGA) of the input motion, as shown in Figure 3a, distinct failure points can be identified. The data indicate that as the input PGA exceeded 0.4g, a significant drop occurred in the amplification factor at a relative height of 0.6 (accelerometer A3). Subsequently, as the PGA surpassed 0.5g, a similar drop was observed at a relative height of 0.9 (accelerometer A4). This sequence suggests a progressive failure mechanism that initiates at a lower elevation and propagates upward as shaking intensity increases.

Following identification of the failure locations and their corresponding PGA thresholds, a more detailed analysis of the accelerometer time histories was conducted to determine the exact timing and energy of these events. By scrutinizing the records for accelerometers A3 and A4 from test T03, it was determined that failure was initiated at 45.8 seconds and 32.8 seconds from the start of shaking, respectively. The cumulative Arias Intensity, which quantifies the total seismic energy imparted to the model, was then calculated up to these specific moments. As illustrated in Figure 4, the corresponding Arias intensities required to trigger failure were found to be 25.53 m/s at the relative height of 0.6 and 9.71 m/s at the relative height of 0.9. This detailed analysis enables a quantitative comparison of the energy required to induce failure across different experimental conditions.

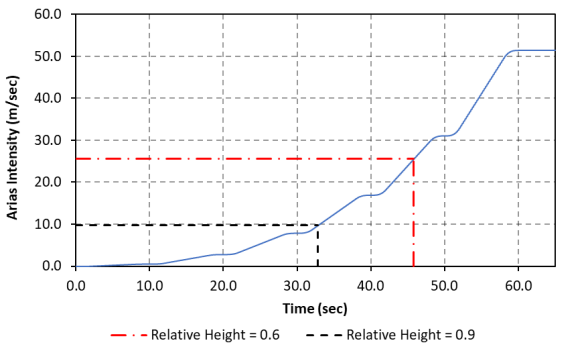

Figure 4. Arias intensity required for failure at relative heights of 0.6 and 0.9 for test "T03"

3.3 *Crest settlement at failure*

The analysis of crest settlement provides a critical measure of the overall seismic performance and permanent deformation of the slope models. For each test, the settlement was quantified as the cumulative vertical displacement measured at the slope crest at the conclusion of each loading cycle, corresponding to a specific peak ground acceleration (PGA). This approach allows for a systematic evaluation of how permanent deformation accumulates as shaking intensity increases.

To illustrate the key features of the observed deformation behavior, the results from the Group 2 tests, which focused on the influence of surcharge loading, are presented in Figure 5. A primary finding from these tests is that applying a surcharge load at the crest significantly exacerbates settlement. The data clearly demonstrate that as the magnitude of the surcharge increases, the onset of significant settlement occurs at considerably lower levels of ground shaking. Furthermore, the ultimate crest settlement recorded at the end of the test is substantially larger for slopes subjected to higher surcharge loads. This indicates that the additional driving forces imposed by the surcharge reduce the slope's capacity to resist seismically induced deformation.

Quantitatively, the effect of the surcharge is pronounced. In the baseline case with no surcharge applied, measurable settlement was not initiated until the input PGA exceeded 0.5g. In contrast, when a surcharge of 1 kPa was applied, settlement began at a much lower threshold of 0.3g PGA. For the test involving a 1.5 kPa surcharge, the onset of settlement was observed at a PGA of 0.4g. These results underscore the critical role that surcharge loading plays in controlling the initiation and magnitude of permanent crest settlements during seismic events.

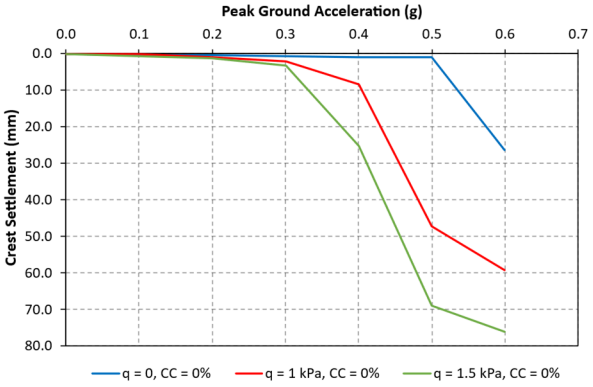

Figure 5. Progression of crest settlement for group (2) tests

4 DISCUSSION

This section highlights the effects of both applied surcharge and cement content on the dynamic behaviour of the tested slopes. Since we are concerned with the global failure of the slope, only the critical condition will be considered for describing the initiation of failure. In other words, the slope is said to have failed as soon as failure occurs at any relative height of the slope. The effects of the applied surcharge and cement content will be assessed using the energy required to initiate failure and the progression of crest settlement. To ensure consistency, the settlement for each test was considered as that occurring after the 0.6g cycle. In general, this experimental testing program demonstrates that increasing the applied surcharge resulted in earlier slope failure initiation and increased crest settlement. On the contrary, increasing the cement content delayed the onset of failure, limited failure to the upper slope, and reduced the resulting crest settlement. It is also worth noting that slopes

with a cement content of 3% did not fail under all applied surcharges for the given ground shaking and are therefore not mentioned in this section.

4.1 *Effect of applied surcharge*

The slope stability is significantly reduced by increasing the applied surcharge. As shown in Figure 6, the arias intensity required to initiate failure drops by 58%, 54%, and 45% for slopes with cement contents of 0%, 1%, and 2%, respectively, as the surcharge increases from 0 to 1.5 kPa. Notably, the decrease in stability is higher for the uncemented slopes than the cemented ones.

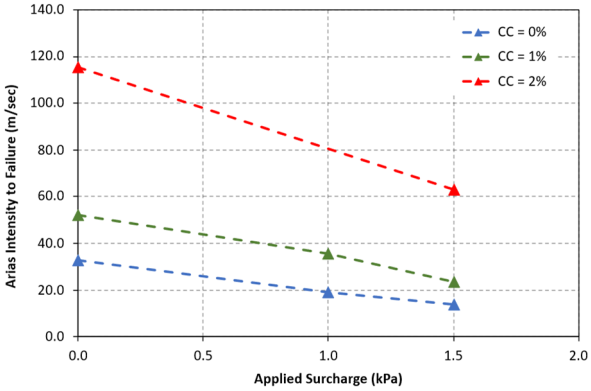

Figure 6. Variation of Arias intensity required to initiate failure with applied surcharge

Crest settlement increases as the slope is subjected to higher surcharge values. As shown in Figure 7, the settlement at the end of the 0.6g cycle for the uncemented slope increased from 26.7 mm to 68.7 mm as the surcharge increased from 0 to 1.5 kPa. As cement is introduced, the effect of the surcharge on the resulting crest settlement becomes lower, and no settlements are observed at all surcharge values when a cement content of 3% is used.

4.2 *Effect of cement content*

Adding cement enhances the strength of the slope material, as indicated by the greater energy required to cause failure and lower crest settlements. Figure 8 shows the increase in Arias intensity required to initiate failure as the cement content is increased from 0 to 2%. The figure shows that the intensity required to failure increases exponentially with increasing cement content, contrary to the linear trends observed for the effect of surcharge loading. This is highly beneficial for slope design, as it implies that the additional stability gained by adding cement can easily offset the increased instability caused by higher surcharge loadings. Since no test was conducted at a cement content of 2% with a surcharge of 1 kPa, the Arias intensity at failure for such a condition was interpolated. Also, no failure was observed as the cement content was increased to 3% under any applied surcharge. Therefore, any predictions of failure under such conditions would require extrapolation from the available results.

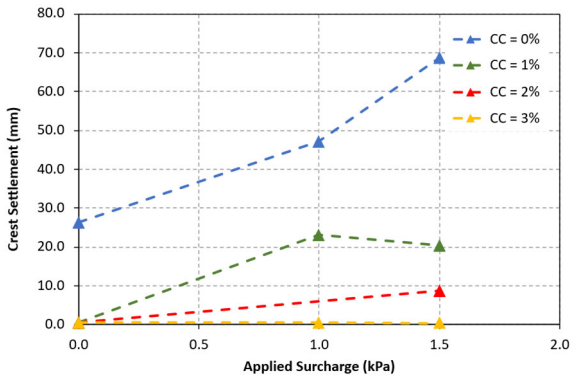

Figure 7. Variation of crest settlement after 0.6g with applied surcharge

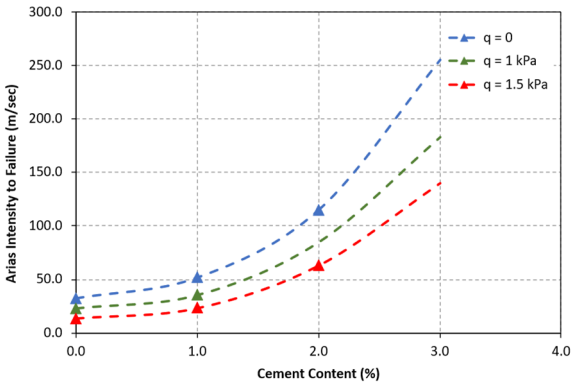

Figure 8. Variation of Arias intensity required to initiate failure with cement content

Figure 9 shows the reduction in resulting crest settlement with increasing cement contents for slopes subjected to different surcharge values. When no surcharge is applied, settlements only occur for the uncemented slope, while the cement content used (1%) is capable of preventing any deformation. As a surcharge is applied, the settlement of the uncemented slopes increases considerably, but gradually decreases as cement is introduced, until no settlement occurs at a cement content of 3%. Therefore, the effect of cement content becomes more relevant as the slope is subjected to higher surcharge values.

5 CONCLUSIONS

This study examined the dynamic behavior of cement-stabilized sandy slopes under seismic loading through a series of 1-g shake-table experiments. The influence of varying cement content and crest surcharge loading was assessed through acceleration amplification trends, crest settlement measurements, and the Arias intensity required to initiate failure. The results showed that cement stabilization notably improves slope performance by delaying the onset of failure, reducing crest displacement, and confining failure to the upper zones of the slope. Even at low cement contents, such as 1% and 2%, a substantial increase in slope resistance was observed, whereas a 3% cement content prevented failure under all tested surcharge conditions.

Conversely, increasing surcharge loading led to earlier slope failure and larger settlements, reflecting a reduction in overall stability. However, the destabilizing effects of surcharge were significantly mitigated by the addition of cement. The energy required to trigger failure increased exponentially with cement content, in contrast to the linear decrease associated with increasing surcharge, highlighting the

efficiency of chemical stabilization in enhancing seismic resistance. These findings suggest that Portland cement can offer a cost-effective and practical alternative to conventional mechanical reinforcement methods, particularly in projects where moderate slope steepening is required and economic or spatial constraints limit the use of more complex systems.

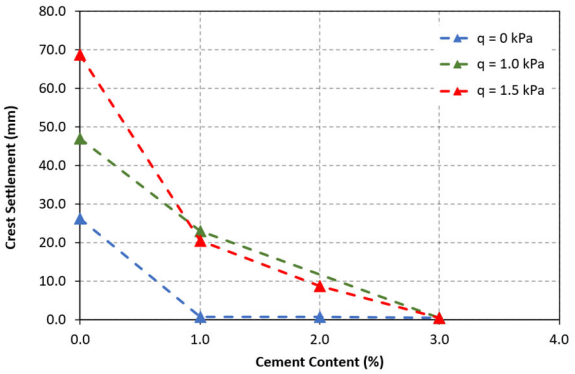

Figure 9. Variation of crest settlement after 0.6g with cement content

6 REFERENCES

Ayazi, M.F. and Tangri, A. (2022). Stabilization of soil nailed slope by flexible materials. *Materials Today: Proceedings*, 49, pp.1950–1955. https://doi.org/10.1016/j.matpr.2021.08.134.

Consoli, N.C., Foppa, D., Festugato, L., and Heineck, K.S. (2007). Key Parameters for Strength Control of Artificially Cemented Soils. *Journal of Geotechnical and Geoenvironmental Engineering*, 133(2), pp.197–205. https://doi.org/10.1061/(asce)1090-0241(2007)133:2(197).

Ghanem, A. (2023). *Studying the Effect of Chemical Stabilization using cement on the Dynamic Behaviour of Slopes using 1-G Shake Table Tests*. Cairo University, M.Sc. Thesis, 129p.

Hazari, S., Ghosh, S., and Sharma, R.P. (2020). Experimental and Numerical Study of Soil Slopes at Varying Water Content Under Dynamic Loading Condition. *International Journal of Civil Engineering*, 18(2), pp.215–229. https://doi.org/10.1007/s40999-019-00439-w.

Iai, S. (1989). Similitude for Shaking Table Tests on Soil-Structure-Fluid Model in 1g Gravitational Field. *Soils and Foundations*, 29(1), pp.105–118. https://doi.org/10.3208/sandf1972.29.105.

Madhavi Latha, G., and Nandhi Varman, A.M. (2014). Shaking table studies on geosynthetic reinforced soil slopes. *International Journal of Geotechnical Engineering*, 8(3), pp.299–306. https://doi.org/10.1179/1939787914y.0000000043.

Mollaei, R., Yazdandoust, M., and Askari, F. (2022). Seismic evaluation of helical soil-nailed walls using shaking table testing. *Soil Dynamics and Earthquake Engineering*, 163, 107331. https://doi.org/10.1016/j.soildyn.2022.107331.

Rios, S. (2011). *A General Framework for the Geomechanical Characterisation of Artificially Cemented Soil.* Universidade do Porto, Programa Doutoral em Engenharia Civil, 334p. https://hdl.handle.net/10216/119663

Saxena, S.K., Avramidis, A.S., and Reddy, K.R. (1988). Dynamic moduli and damping ratios for cemented sands at low strains. *Canadian Geotechnical Journal*, 25(2), pp.353–368. https://doi.org/10.1139/t88-036.

Shooshpasha, Issa, and Shirvani, Reza Alijani (2015). Effect of cement stabilization on geotechnical properties of sandy soils. *Geomechanics and Engineering*, 8(1), pp.17–31. https://doi.org/10.12989/GAE.2015.8.1.017.

Wang, Y.H. and Leung, S.C. (2008). Characterization of Cemented Sand by Experimental and Numerical Investigations. *Journal of Geotechnical and Geoenvironmental Engineering*, 134(7), pp.992–1004. https://doi.org/10.1061/(asce)1090-0241(2008)134:7(992).

Yang, B., Gao, F. and Jeng, D. (2018). Failure mode and dynamic response of a double-sided slope with high water content of soil. *Journal of Mountain Science*, 15(4), pp.859–870. https://doi.org/10.1007/s11629-017-4616-4.

Zhou, Z., Lei, J., Shi, S., and Liu, T. (2019). Seismic Response of Aeolian Sand High Embankment Slopes in Shaking Table Tests. *Applied Sciences*, 9(8), p.1677. https://doi.org/10.3390/app9081677.